Elastic-skinned gravity currents

Anja Slim and Neil Balmforth

Department of Mathematics, University of British Columbia

Introduction

We investigate a layer of very viscous fluid that flows down a uniform slope due to gravity. However, instead of the usual free surface, the fluid is covered by an elastic plate.

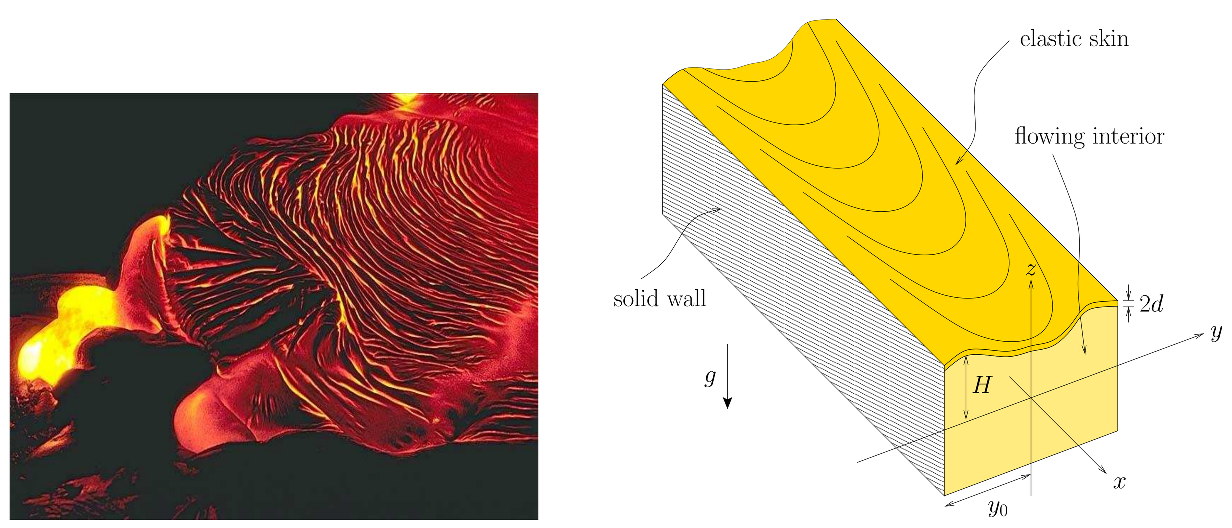

Figure 1: (a) 'Ropy' pahoehoe lava. (b) The configuration studied:

A pahoehoe lava flow may be crudely modelled by such an elastic-skinned gravity current: as a flow advances, it solidifies and forms a crust at the surface whilst remaining molten in the interior. Many such flows exhibit a complex surface structure because of the multitude of stresses acting upon them; an example is shown in figure 1*a*. As an idealization of the wrinkling process, we present a theoretical model describing a viscous fluid flowing down an incline beneath an elastic skin, and apply it to the simple geometry shown in figure 1*b*. The model consists of Stokes equations for the fluid coupled to the nonlinear Föppl–von Kármán plate equations for the skin.

The governing equations

A duct of square cross-section, with half-width and -depth y_0, is inclined at an angle $\theta = 45°$ to the horizontal. The side walls and inclined plane are solid; the upper surface is an elastic plate of half-thickness d, Young's modulus E and Poisson ratio ν. Fluid, of viscosity μ and density ρ, flows under the force of gravity alone. The x-direction is directed down-slope, the y-direction across-slope and the z-direction perpendicular to the slope.

We present the governing equations in non-dimensional form where lengths have been rescaled by y_0, velocities by $U = \rho g \cos\theta y_0^2/\mu$, time by y_0/U, fluid stresses by $\rho g \cos\theta y_0$ and elastic stresses by $2dE/(1-\nu^2)$. We set

$$\delta = d/y_0 \qquad G = \rho g y_0^2 (1-\nu^2)\cos\theta/2dE,$$

where the latter measures the relative strength of the shear forces induced by the fluid on the plate compared to the elastic forces.

The fluid

The interior flow is assumed inertialess and incompressible, thus

$$\nabla\cdot\mathbf{u} = \mathbf{0}, \qquad -\boldsymbol{\nabla} p + \nabla^2\mathbf{u} + (1,0,-1) = \mathbf{0}, \tag{1}$$

where p is pressure and $\mathbf{u} = (u,v,w)$ the velocity field. The inclined plane and the side walls are no-slip: $\mathbf{u} = \mathbf{0}$ on $z = -1$ and $y = \pm 1$.

The crust

The crust is modelled as a thin, Hookean elastic plate. Its upper face is free while the fluid exerts a traction, $\mathbf{t} = (t_X, t_Y, t_Z)$ on its lower face, generating in-plane stresses and displacements which in turn induce buckling. The Föppl–von Kármán equations are the simplest plate equations that can capture such behaviour.

The plate displacement is denoted by the vector, (ξ,η,ζ), each component of which is a function of the undeformed position, (X,Y), of the plate (located on the $Z=0$ plane); after deformation, the plate is located at the position $(X+\xi, Y+\eta, \zeta)$. Assuming deformations are slow, so elastic accelerations can be neglected, the in-plane and out-of-plane motions are governed by

$$\nabla\cdot\mathsf{N} = G\begin{pmatrix} t_X \\ t_Y\end{pmatrix}, \qquad \tfrac{1}{3}\delta^2\nabla^4\zeta = -Gt_Z + \nabla\cdot(\mathsf{N}\cdot\boldsymbol{\nabla}\zeta), \tag{2}$$

respectively, where the in-plane stresses, N, and associated nonlinear in-plane strains, e, are given by

$$\mathsf{N} = \nu\,\mathrm{tr}\,(\mathsf{e})\,\mathsf{I} + (1-\nu)\mathsf{e}, \qquad \mathsf{e} = \frac{1}{2}\left(\boldsymbol{\nabla\xi} + \boldsymbol{\nabla\xi}^T + \boldsymbol{\nabla}\zeta\boldsymbol{\nabla}\zeta\right). \tag{3}$$

At the lateral edges of the plate we impose clamped boundary conditions $\xi = \eta = \zeta = \zeta_Y = 0$ on $Y = \pm 1$.

Matching conditions

A key assumption of the Föppl–von Kármán equations is that in-plane displacements are small. As a result, the relation between the two coordinate systems, $\mathbf{x}$ and $\mathbf{X}$ can be simplified: $(x,y) = (X,Y) + (\xi,\eta) \approx (X,Y)$ and $\zeta(X,Y,t) \approx \zeta(x,y,t)$. That is, we may ignore any difference between the two coordinate systems.

Continuity of velocity now requires (ignoring the production of crust and under the assumptions of Föppl–von Kármán)

$$\xi_t = u, \qquad \eta_t = v, \qquad \zeta_t = w, \tag{4}$$

and the matching of the stresses implies that

$$t_X = \hat{\mathbf{t}}_\mathbf{1}\cdot\sigma\cdot\hat{\mathbf{n}}, \qquad t_Y = \hat{\mathbf{t}}_\mathbf{2}\cdot\sigma\cdot\hat{\mathbf{n}}, \qquad t_Z = \hat{\mathbf{n}}\cdot\sigma\cdot\hat{\mathbf{n}}, \tag{5}$$

where $\hat{\mathbf{n}}$ is the unit normal to the base of the plate, and $\hat{\mathbf{t}}_j$ ($j = 1$ and 2) are the corresponding tangents aligned with the $x-$ and $y-$axes, respectively.

Wrinkling instability

We consider a base state with no out-of-plane displacement of the elastic plate, no variation in x and having $v = w = 0$. The solution of the system (1)–(5) is shown graphically for the down-slope velocity and down-slope displacement in figure 2*a* and *b* respectively. The velocity is identical to that found at zero Reynolds number in a rectangular duct, while the down-slope displacement in the plate is almost parabolic, with maximal shear in the plate at its lateral edges.

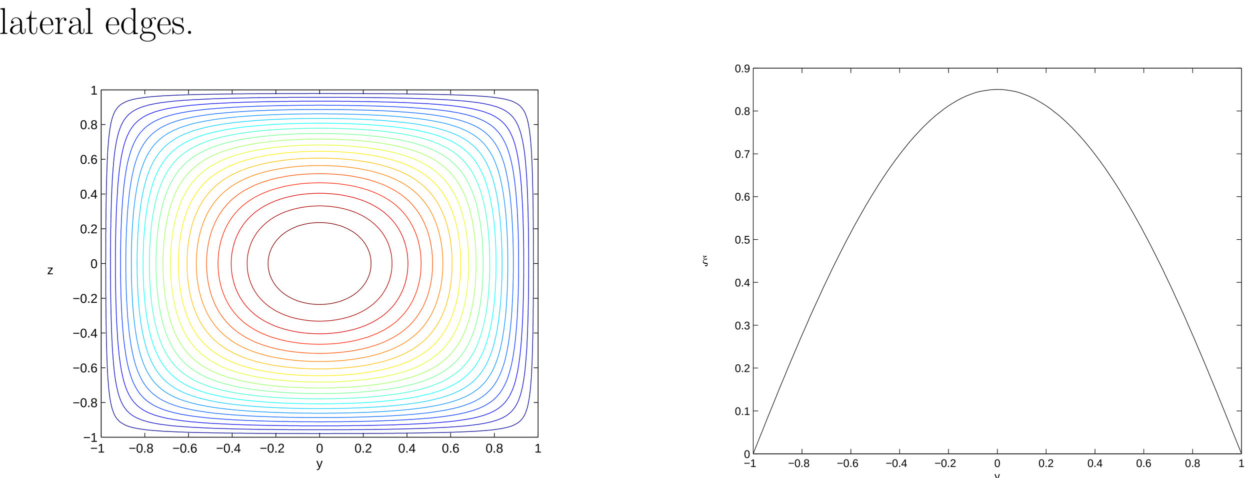

Figure 2: The base state down-slope (a) fluid velocity contours and (b) plate displacement for $\nu = 0.3$ and $G = 1$.

Perturbation

To consider the out-of-plane displacement induced by this base flow, we perturb the base state by an infinitesimal amount decomposed into a normal mode proportional to $e^{ikx - i\omega t}$. Using 0 (1) superscripts to denote the base (perturbation) values, we find the equations governing the perturbation become

$$\tfrac{1}{3}\alpha\delta^2\left(\zeta^{(1)}_{yyyy} - 2k^2\zeta^{(1)}_{yy} + k^4\zeta^{(1)}\right) + G\zeta^{(1)} - ik(1-\nu)\xi^{(0)}_y\zeta^{(1)}_y - \alpha G w^{(1)}_z - Gp^{(1)} = 0,$$

for the plate with $\zeta^{(1)} = \zeta^{(1)}_y = 0$ at $y = \pm 1$,

$$\nabla\cdot\mathbf{u}^{(1)} = \mathbf{0}, \qquad \mathbf{0} = -\boldsymbol{\nabla} p^{(1)} + \nabla^2\mathbf{u}^{(1)},$$

with conditions $\mathbf{u}^{(1)} = \mathbf{0}$ on $y = \pm 1$, $z = -1$ and

$$u^{(1)} + u^{(0)}_z\Big|_{z=1}\zeta^{(1)} = 0, \qquad v^{(1)} = 0, \qquad w^{(1)} = -i\omega\zeta^{(1)} \qquad \text{on } z = 1.$$

We solve the perturbation equations numerically using a Chebyshev collocation scheme.

Sample growth rates of the most unstable modes are shown in figure 2. Above a critical value of the gravitational parameter, G, a finite window of unstable wavenumbers is found at moderate k. Both short- and long-waves are stabilized by the bending stiffness of the plate, which prevents buckling in the x- and y-directions respectively. The mode with largest growth rate is symmetric. The structure of the modes described below implies that the displacement in the central region decreases as k increases, thus the symmetric and antisymmetric modes have almost identical growth rates as k becomes large.

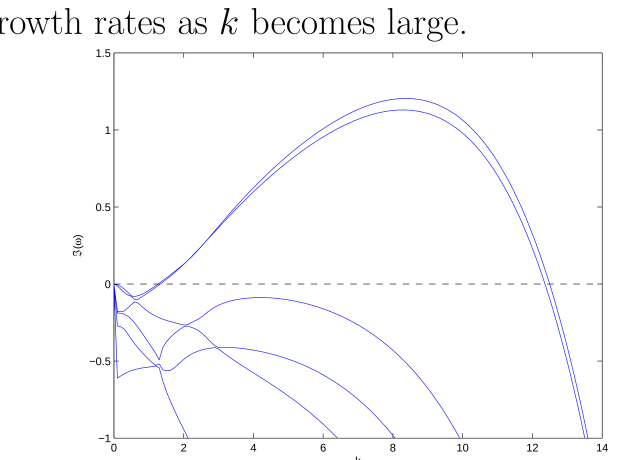

Figure 3: The growth rate, $\Im(\omega)$, as a function of wavenumber for the most unstable modes for $G = 3$, $\delta = 0.1$ and $\nu = 0.3$.

Mode profiles for the most unstable mode at approximately the most unstable wavenumber are shown in figure for $G = 3$, $k = 8$ and $\delta = 0.1$. The largest amplitude deflection occurs away from the centre-line and edges. This is to be expected since the base-state stress is zero at the centre, while the clamped boundary conditions prevent deformation at the edges. Where k and G are small the maximum amplitude is at the centre-line, while for increasing G or k the maximum is progressively closer to the clamped edges. The induced flows are confined to a relatively thin layer close to the plate.

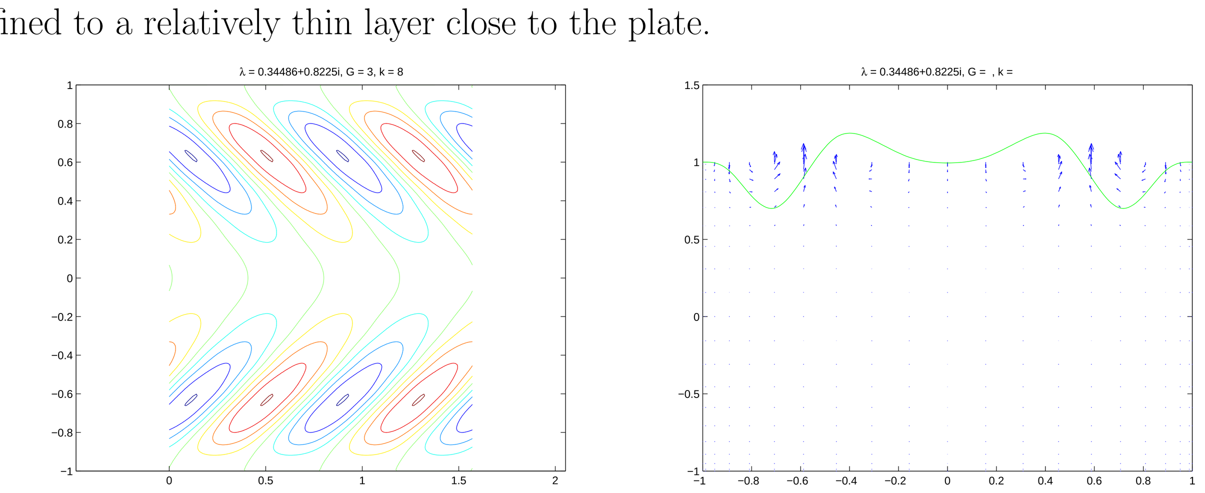

Figure 4: (a) The out-of plane perturbation profiles as functions of x and y for the most unstable mode. (b) Cross-sections of the out-of-plane displacement (exaggerated) and cross-sectional velocity fields. The parameters are $G = 3$, $k = 8$, $\delta = 0.1$ and $\nu = 0.3$.

Discussion

We have presented a model for describing an elastic-skinned gravity current that is capable of capturing flow-induced wrinkling. We have investigated the linear stability of a simple geometry, however slight modifications may also be applied to consider fingering of the front, flow-induced compression at the front and more complex geometries in which shear induces buckling.